

EFFECT OF RADIATIVE TRANSPORT ON THE EVOLUTION OF JUPITER AND SATURN

T. GUILLOT¹

Observatoire de la Côte d'Azur, CNRS/URA 1362, BP 229, 06304 Nice Cedex 4, France

G. CHABRIER

Centre de Recherche Astrophysique, UHR CNRS 142, Ecole Normale Supérieure, 69364 Lyon Cedex 07, France

D. GAUTIER

DESPA, Observatoire de Paris, 5 pl J. Janssen, 92195 Meudon Cedex, France

AND

P. MOREL

Observatoire de la Côte d'Azur, CNRS/URA 1362, BP 229, 06304 Nice Cedex 4, France

Received 1994 December 12; accepted 1995 March 9

ABSTRACT

Conventional evolutionary models for Jupiter and Saturn, which assume convection throughout the *entire* planet interior, yield ages of 5.1 Gyr for Jupiter and 2.6 Gyr for Saturn. Even though the discrepancy for Saturn can be explained by the additional energy source due to a phase separation of helium, it seems difficult to reconcile the age of fully convective Jovian models with the age of the solar system, i.e., 4.5 Gyr.

It has been recently shown that these planets are probably not fully convective, but retain a stable radiative window near the surface. We present new evolutionary models for these two planets, which do include the aforementioned possibility of radiative transport in the molecular hydrogen-helium envelope. These calculations yield ages of 4.2 Gyr for Jupiter and 2.4 Gyr for Saturn. We show that the importance of the radiative window was larger in the past than now, so that the ratio of the radiative to the adiabatic gradient in the radiative region increases with time. This speeds up the cooling with respect to a fully adiabatic planet.

Since the interiors of the new Jupiter and Saturn models are significantly cooler than the adiabatic ones, it is likely that immiscibility of helium occurs in both planets. That provides a natural explanation for the observed helium depletion in their atmospheres and the fact that the ages inferred from homogeneous evolution models of these two planets are smaller than the age of the solar system.

Subject headings: convection — planets and satellites: individual (Jupiter, Saturn) — radiative transfer

1. INTRODUCTION

The accurate description of the interior structure and the evolution of Jupiter and Saturn is a key to the understanding of the formation of the solar system. In particular, since the giant planets are relics of the primitive solar nebula, one can infer the chemical composition of this nebula from the one presently observed in the atmospheres of these planets. This requires a very accurate description of their internal structure and evolution. The evolutionary models are constrained by the observed present radii, effective or surface temperatures, and luminosities of each planet, and by the age of the solar system, accurately determined by datings of meteorites (see, e.g., Göpel, Manhès, & Allègre 1994).

The formation and evolution of the giant planets can be characterized by three phases: (a) the accretion of a core formed by refractory materials; (b) the rapid contraction of a hydrogen-helium envelope characterized by a strong increase of temperature at roughly constant luminosity; (c) a quasi-static evolution phase, due to the increasing incompressibility of the envelope, and during which both temperature and luminosity decrease with time whereas the radius of the planets remains nearly constant. The duration of the first two phases is almost negligible compared to this third phase (see, e.g., Lissauer 1987; Pollack & Bodenheimer 1989). The aim of the present paper is to provide an accurate description of the ongoing quasi-static evolution phase for Jupiter and Saturn.

Evolutionary models for Jupiter were first developed by Graboske et al. (1975). These authors considered the planet as a star of approximately $10^{-3} M_{\odot}$ and calculated atmospheric conditions for the evolution which are still used in actual calculations. The same kind of models has been worked out for Saturn by Pollack et al. (1977). A semianalytic model of evolution of Jupiter has been derived by Hubbard (1977). Improved calculations were then conducted by Grossman et al. (1980), for the treatment of the core, and Saumon et al. (1992), who used an improved equation of state and considered the effect of a first-order transition between molecular and metallic hydrogen on the evolution. Except for the original calculation of Graboske et al. (1975), all these works yield similar ages for Jupiter and Saturn, i.e., 4.5–5.3 Gyr and 2–3 Gyr, respectively. The discrepancy between the age of theoretical models of Saturn and the age of the solar system (i.e., ~ 4.5 Gyr) can probably be explained by a phase separation of helium inside the planet, as shown by Stevenson & Salpeter (1977) and Hubbard & Stevenson (1984).

All these calculations assume a *homogeneous* hydrogen-helium envelope. In the evolutionary calculations of Saumon et al. (1992), this envelope is separated into a metallic and a molecular region (with a discontinuity of the entropy but no abundance discontinuity at the transition). Since this paper focuses on the effect of radiative transfer on the evolution, we will use the same assumption. We emphasize, however, that more realistic models should include the presence of helium sedimentation through a molecular-metallic transition or a hydrogen-helium phase separation. An inhomogeneous abun-

¹ Present address: Lunar & Planetary Laboratory, University of Arizona, Tucson, AZ 85721.

dance of helium is required in order to fulfill the constraints of a global protosolar helium abundance ($Y_N = 0.28 \pm 0.02$) and the observed atmospheric abundances ($Y = 0.18 \pm 0.04$ for Jupiter and $Y = 0.06 \pm 0.05$ for Saturn; Gautier & Owen 1989).

The article is organized as follows: in § 2, we describe the evolution and the computational method. The results are presented in § 3 where we compare the internal conditions between adiabatic and nonadiabatic models, at various ages. The evolution of the hydrogen molecular/metallic transition, and of the radiative region are described in terms of the entropy profiles. Section 4 is devoted to a discussion on the possibility of a phase separation of hydrogen and helium in these planets. The conclusions are given in § 5. We present in the Appendix an analytical model of evolution for an "ideal" Jupiter.

2. METHOD

2.1. Physical Inputs

Figure 1 shows present-day models of Jupiter and Saturn, as calculated by Guillot et al. (1994b). We assume that these planets consist in (a) a dense core (formed with refractory species, rocks, and more volatile elements, ices) surrounded by (b) a homogeneous envelope composed mainly of hydrogen and helium, in which hydrogen undergoes a first-order transition from a high-pressure metallic phase to a low-pressure molecular phase (Chabrier et al. 1992; Saumon & Chabrier 1992). We emphasize that the assumption of homogeneity yields present-day models which are not fully consistent with the observations. The problem of the evolution of giant planets assuming an inhomogeneous envelope remains to be done.

The mass of the core, as well as the mass fraction of heavier-than-hydrogen elements (Y_Z) are such that present-day models match the actual radius and gravitational moments J_2 , J_4 , J_6 within less than 2σ (σ being the observational error bar) (Guillot et al. 1994b). These parameters are listed in Table 1.

We used the hydrogen equation of state (EOS) calculated by Saumon & Chabrier (1991, 1992), extended to the hydrogen-helium mixture (Saumon, Chabrier, & Van Horn 1995). We always consider the case where the hydrogen molecular/metallic transition is a first-order (i.e., discontinuous) phase transition (PPT) (Saumon & Chabrier 1992). That yields models in better agreement with the observations than those assuming a continuous transition (Chabrier et al. 1992; Guillot et al. 1994b). The larger uncertainties in this EOS are located (i) near the critical point of the PPT ($P \approx 0.6$ mbar; $T \approx 15,300$ K) and (ii) in the high-pressure, low-temperature region ($P \gtrsim 0.3$ mbar and $T \lesssim 3000$ K). These two regions correspond approximately to the two extremities of our evolution calculations. The EOS for the core has been calculated by Hubbard & Marley (1989). Its accuracy is sufficient in view of the smallness of the core.

TABLE 1
PARAMETERS FOR THE MODELS OF
JUPITER AND SATURN

Planet	Model	Y_Z	$M_{\text{core}}/M_{\oplus}$
Jupiter	{ Adiabatic	0.311	6.6
	{ Nonadiabatic	0.271	8.0
Saturn	{ Adiabatic	0.339	18.1
	{ Nonadiabatic	0.295	20.1

We compare evolutionary models assuming convection throughout the *entire* hydrogen-helium envelope (see "adiabatic models" in Fig. 1) with models which take into account the finite radiative opacities in the outermost layers (see "nonadiabatic models" in Fig. 1). The opacities are taken from Guillot et al. (1994a). As discussed by the authors, these opacities are certainly underestimated (due to lacks in the opacity data banks, the presence of polyatomic molecules, ..., etc.). These uncertainties are probably larger for earlier, hotter models since the calculations are based on the assumption that the abundance of water, methane, and ammonia is essentially constant, i.e., the thermochemical equilibrium involving these molecules is not calculated. This assumption is based on the calculations of Barshay & Lewis (1978) and Fegley & Lodders (1994), which refer to present-day conditions in Jupiter. For early models of the giant planets, the chemical equilibrium is probably substantially different and should be recalculated. However, as discussed in the Appendix, the initial conditions, for which these uncertainties are the largest, have a very small effect on the evolution. Moreover, as will be shown in § 3, the inner temperature varies very slowly with time after 1 Gyr. The modifications in the chemical abundances should be small between 1 Gyr and the present time. Therefore, we expect the effect of the aforementioned approximation to remain marginal.

The equations describing the internal structure and evolution of giant planets are described in Guillot et al. (1994b) and Guillot & Morel (1995). Here, we include rotation to the lowest order in angular velocity ω only, so that the hydrostatic equilibrium equation becomes

$$\frac{\partial P}{\partial M} = -\frac{GM}{4\pi R^4} + \frac{\omega^2}{6\pi R}, \quad (1)$$

where all symbols have their usual meaning (see Guillot et al. 1994b). Higher order rotation terms can be neglected, as they contribute to less than 1% in equation (1) during the entire evolution process, for both Jupiter and Saturn (see Guillot & Morel 1995). This is small compared to the uncertainties related to the physical inputs (atmosphere, EOS, ..., etc.), and to the differential rotation.

We also neglect the presence of any radioactive sources in the hydrogen-helium envelope, since their contribution to the total luminosity is less than 1%. Therefore, the equation of energy conservation in the envelope reads

$$\frac{\partial L}{\partial M} = -T \left(\frac{\partial \tilde{S}}{\partial t} \right), \quad (2)$$

where L is the intrinsic luminosity and \tilde{S} is the entropy per unit mass (specific entropy).

As described in Guillot & Morel (1995), we assume that the core is isothermal. Moreover, we do not integrate equation (2) in the core. Instead, we fix the luminosity at the surface of the core as the sum of the luminosity due to radioactive decay and to the cooling of the core (the neglect of the contraction luminosity yields an error of about 10%):

$$L_{\text{core}} = L_{\text{radioactive}} - M_{\text{core}} C_v \frac{\partial T}{\partial t}. \quad (3)$$

We used the values $L_{\text{radioactive}} = 2 \times 10^{20} (M_{\text{core}}/M_{\oplus})$ ergs s^{-1} and $C_v = 10^7$ ergs $K^{-1} g^{-1}$. $L_{\text{radioactive}}$ corresponds roughly to the radioactive decay of chondrites. The value of the heat capacity is obtained by averaging the ice and heavy atoms

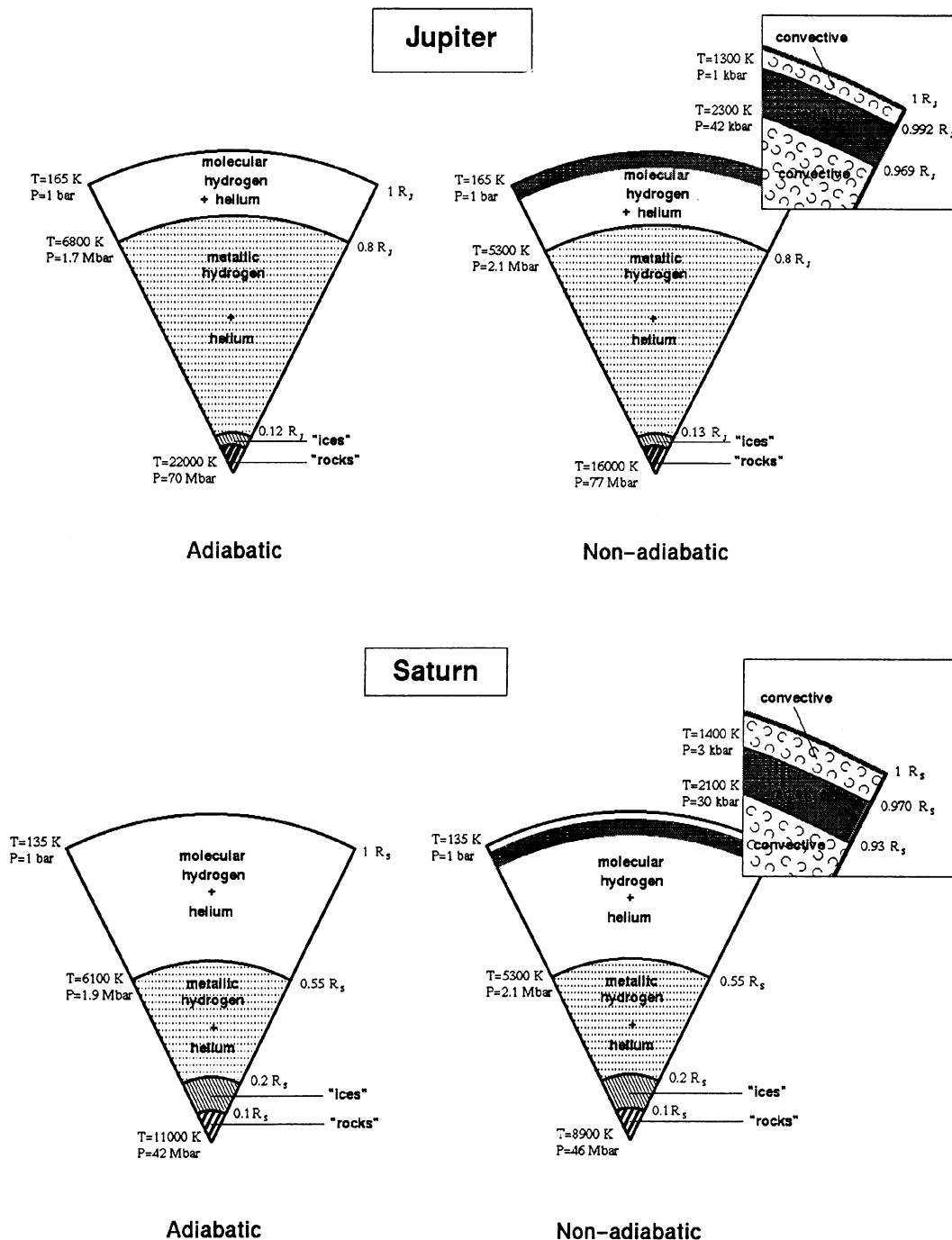


FIG. 1.—Present models of Jupiter and Saturn, calculated (a) assuming a fully convective hydrogen-helium envelope (adiabatic models); (b) including the presence of a radiative window in the molecular envelope (nonadiabatic models) (from Guillot et al. 1994b).

(iron, silicates, ...) heat capacities (see Hubbard & MacFarlane 1980).

The boundary condition at the “surface” of the planet (i.e., at the 1 bar level) is chosen as in Hubbard (1977) and Saumon et al. (1992), based on model atmospheres by Graboske et al. (1975):

$$T_{1\text{bar}} = K T_{\text{eff}}^{1.244} g^{-0.167}, \quad (4)$$

where g is the gravity at the surface ($g \approx 2600 \text{ cm s}^{-2}$ and $g \approx 1100 \text{ cm s}^{-2}$ for present Jupiter and Saturn, respectively),

T_{eff} is the effective temperature (such that $4\pi R^2 \sigma T_{\text{eff}} = L_{\text{int}} + L_{\odot}$, the sum of the intrinsic luminosity and the luminosity due to solar heating), and K is a constant of normalization. This constant is chosen such that, for the actual radius and luminosity, the 1 bar temperature fits the observed value. Actual observations for these quantities (see Lindal 1992 and references therein) yield $K = 1.519$ for Jupiter and $K = 1.511$ for Saturn.

We assume that the mass, the angular velocity, and the solar heat flux input of the planet at the 1 bar level are constant

during the quasi-static evolution. The variations of these quantities during this phase are small and barely affect the results (see the small variations of the radius in Figures 4–7 below). For the same reason (small variations of R), assuming a constant *angular momentum* instead of constant angular velocity, affects only the very early contraction phase.

2.2. Computational Method

As in stellar evolution, the numerical problem is a two-point boundary initial value problem, i.e., an initial value (Cauchy) problem coupled with a two-point boundary (Dirichlet) problem. The latter is described in Guillot & Morel (1995). We focus here on the Cauchy problem.

For the initial solution, we first calculate a static model with the relation:

$$\frac{\partial \tilde{S}}{\partial t} \equiv c_1, \quad (5)$$

where c_1 is chosen such that the luminosity of this initial model is approximately equal to 1000 times the actual luminosity (this is a typical value expected at the end of the rapid contraction phase—see Pollack & Bodenheimer 1989). Though arbitrary, equation (5) describes a fully isentropic model close to the models sought. In fact, this relation would be exact for fully convective models with no first-order phase separation.

A second static model is calculated with a constant $c_2 = 1.1c_1$. The time step for the evolution process is then given by

$$\Delta t \approx \left\langle \frac{\tilde{S}_2 - \tilde{S}_1}{c_1} \right\rangle_M. \quad (6)$$

The average value for the entropy is just an approximation, since these models are not necessarily isentropic.

A Newton-Raphson iterative algorithm is used for solving the nonlinear set of discretized equations. For the first iteration of each time step we use an estimate of $(\partial \tilde{S}/\partial t)_{t+\Delta t}$ given by a linear extrapolation of the former solutions $(\partial \tilde{S}/\partial t)_t$ and $(\partial \tilde{S}/\partial t)_{t-\Delta t}$, as well as extrapolations of the temperature and the luminosity. For the next iterations, equation (2) is written, using finite differences, as a fully implicit equation:

$$\left(\frac{\partial L}{\partial M} \right)_{t+\Delta t} = -T_{t+\Delta t} \frac{\tilde{S}_{t+\Delta t} - \tilde{S}_t}{\Delta t}. \quad (7)$$

This numerical scheme has been chosen for its stability, even though it is less accurate than schemes based on a centered method.

The reliability of this method has been tested with the simple model described in the Appendix. Moreover, we have verified that a different choice of the initial constants (as soon as the luminosity of the initial model is high enough) does not alter the final results. The overall calculation has been performed using the numerical code CEPAM (see Guillot & Morel 1995).

3. RESULT: THE QUASI-STATIC EVOLUTION PHASE OF JUPITER AND SATURN

3.1. Comparison of the Internal Conditions

Figures 2 and 3 show the time variations of the pressure, the temperature, the density, and the luminosity profiles of Jupiter and Saturn. The increase of the pressure and density is small, whereas the decrease of the temperature and the luminosity is much more significant. The relatively small variations of the

pressure and density profiles are essentially due to degeneracy in a large part of the interior of the planet. The decrease of the temperature and the luminosity is controlled by the atmosphere and is essentially exponential.

Adiabatic models are always hotter and have a more important contraction than nonadiabatic models, as shown on Figure 2 for Jupiter, and on Figure 3 for Saturn. Although adiabatic and nonadiabatic models have not been calculated with the same initial conditions, this is inconsequential to the final results (see Appendix). The same results have been found using an adiabatic solution during the first 0.5 Gyr and then switching to a nonadiabatic calculation.

In the case of Saturn, models which are compatible with present-day observations were reached very rapidly compared to the age of the solar system. Therefore, we have stopped the evolution process before 4 Gyr for this planet. This demonstrates the necessity of including an extra energy source in Saturn's cooling.

In each figure, the position of the PPT is indicated by the density discontinuity. The flattening of the temperature profiles for early adiabatic models is due to the proximity of the critical point of the PPT, where $V_{ad} \approx 0$ (see Saumon, Chabrier, & Van Horn 1995). The nonadiabatic models, cooler than the adiabatic ones, are found to be always subcritical. The radiative region (near the surface) is too narrow to be seen on these graphs. The structure of the core is not shown, for clarity.

3.2. Ages

By definition, all our initial models correspond to $t = 0$. The age of a given model is the value of t for which the radius, temperature, and luminosity fit the present values. This age corresponds to the duration of the quasi-static phase of evolution. The core accretion phase is comparatively short, from 10^{-3} Gyr (Hayashi, Nakazawa, & Nakagawa 1985; Lissauer 1987) to 0.1 Gyr (Safronov 1972; Safronov & Ruzminkaia 1985). The subsequent hydrodynamic collapse (Wuchterl 1991) or rapid contraction (Pollack & Bodenheimer 1989) of the hydrogen-helium envelope is even more rapid. Therefore, the ages calculated here should be close to the age of the solar system determined from isotropic dating of meteorites.

The evolution of all our models is characterized by a slow contraction and a more rapid cooling, as shown on Figures 4 to 7. Furthermore, the variations of the radius, the temperature, and the luminosity are much more important during the first billion years after the formation of the planet than from this epoch to now. The present-day conditions are indicated in Figures 4 to 7 by a horizontal dotted line. All the quantities have been normalized to this value. The three curves should cross this value at the same time. It is not exactly the case, since we have neglected the high-order rotation terms in equation (1). However, this leads to an uncertainty on the ages which is always less than 0.2 Gyr.

As shown by Figures 4 and 6, the ages found for adiabatic models of Jupiter and Saturn are in good agreement with the results of Saumon et al. (1992). Following these authors, we also verified that the ages of models calculated with an interpolated EOS (see Guillot et al. 1994b) are close to the ages found here (with differences smaller than 0.2 Gyr), for both adiabatic and nonadiabatic models. The presence of the PPT has little effect on the evolution.

We find that the adiabatic model of Jupiter has an age of 5.1 ± 0.1 Gyr, which is not compatible with the age of the solar system. It can be argued that the relationship between the

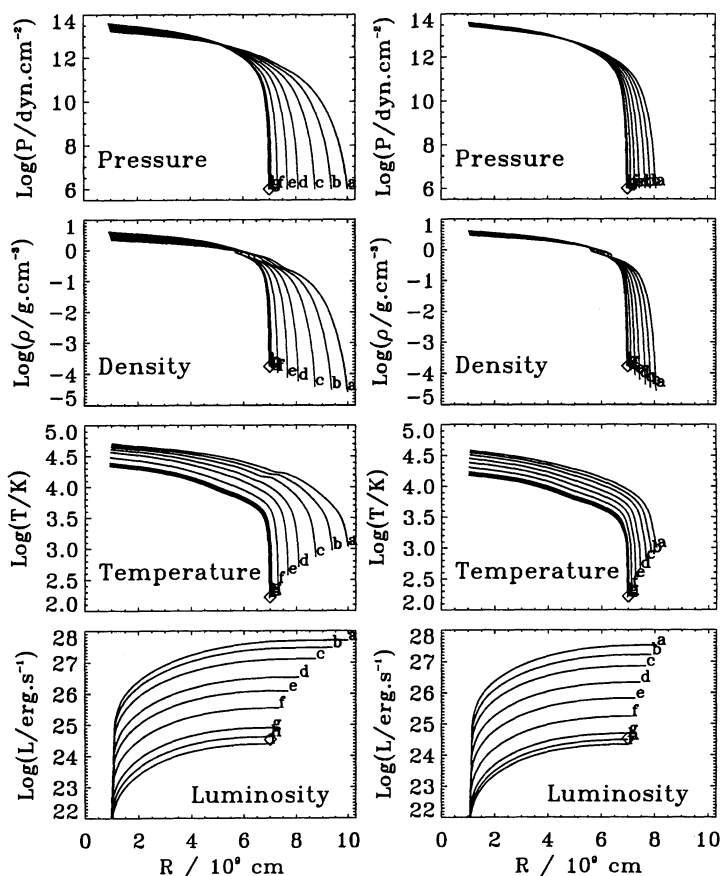


FIG. 2.—Evolution of the internal structure of Jupiter assuming a fully convective envelope (*left*), and for partly radiative models (*right*). The pressure, temperature, density, and intrinsic luminosity are shown as functions of the internal radius. The different curves correspond to ages of: (a) 0.001, (b) 0.01, (c) 0.03, (d) 0.1, (e) 0.3, (f) 1, (g) 3, (h) 4.5, and (i) 6 Gyr. The diamonds indicate the actual “surface” (at the 1 bar level) conditions on Jupiter.

surface and the effective temperature described by equation (4) is very approximate and may explain the discrepancy. This means that, using a similar relation between the surface and the effective temperature, the exponent should be ~ 1 instead of 1.244.² The uncertainty related to the EOS is probably smaller, but is not negligible, either. Recent shock-wave experiments (Holmes, Ross, & Nellis 1995) indicate that the Saumon-Chabrier EOS probably overestimates the temperature for a given pressure along a Jovian adiabat. The ages calculated with this EOS could then possibly be overestimated. However, the sedimentation of helium, which is not taken into account in these models, will increase the age of the models, and thus the discrepancy with the age of the solar system.

On the other hand, our nonadiabatic models of Jupiter are aged 4.2 ± 0.1 Gyr. This is less than the age of the solar system, but this discrepancy can be explained (i) by the fact that we do not take into account helium sedimentation, (ii) by the probably underestimated opacities, (iii) by the uncertainties on equation (4). At any rate, that shows that radiative transport did indeed play an important role in the evolution of Jupiter, and must be included in a proper description of this problem.

² The calculations of Graboske et al. (1975) at high temperatures ($T_{\text{eff}} \sim 600$ K) happen to be in fair agreement with brown dwarf atmospheric models (Burrows et al. 1993). However, equation (4) is a good fit of Graboske et al. results only for effective temperatures below 200 K. Above that limit, the exponent on T_{eff} in equation (4) drops to ~ 0.95 . Taking this into account leads to ages which are smaller by only ~ 0.2 Gyr compared to that calculated using equation (4).

It is well known that the age obtained for *homogeneous* models of Saturn is incompatible with the age of the solar system. In agreement with previous calculations, we find that adiabatic models of this planet are aged 2.6 ± 0.2 Gyr. Non-adiabatic models predict ages about 2.4 ± 0.2 Gyr. Therefore, the presence of a radiative window (i) does not bear as important consequences on the evolution of Saturn as on Jupiter, (ii) does *not* explain the actual luminosity of this planet. As shown by Saumon et al. (1992), the problem is not solved by a first-order transition between molecular and metallic hydrogen. The most probable explanation is the presence of a hydrogen-helium phase separation in the interior of the planet, as suggested by Stevenson & Salpeter (1977).

3.3. Entropy Profiles

Since the equation of energy conservation (eq. [2]) does not contain any heating source, the evolution of the planet is governed by the specific entropy \tilde{S} . This quantity also characterizes the process of energy transport (convective, radiative...).

Since convection in Jupiter and Saturn is quasi-adiabatic, the specific entropy is constant in the convective layers. On the other hand, a *radiative* region is characterized by a *decrease* of entropy toward the interior. At the PPT, there is by definition an entropy jump, which amounts to $\sim 0.6 k_B$ proton⁻¹ (Saumon & Chabrier 1992). The entropy is not calculated in the core.

These features are clearly seen on Figures 8 and 9: from the limit of the core ($M = M_{\text{core}}$) to the surface ($M = M_{\text{tot}}$), we can

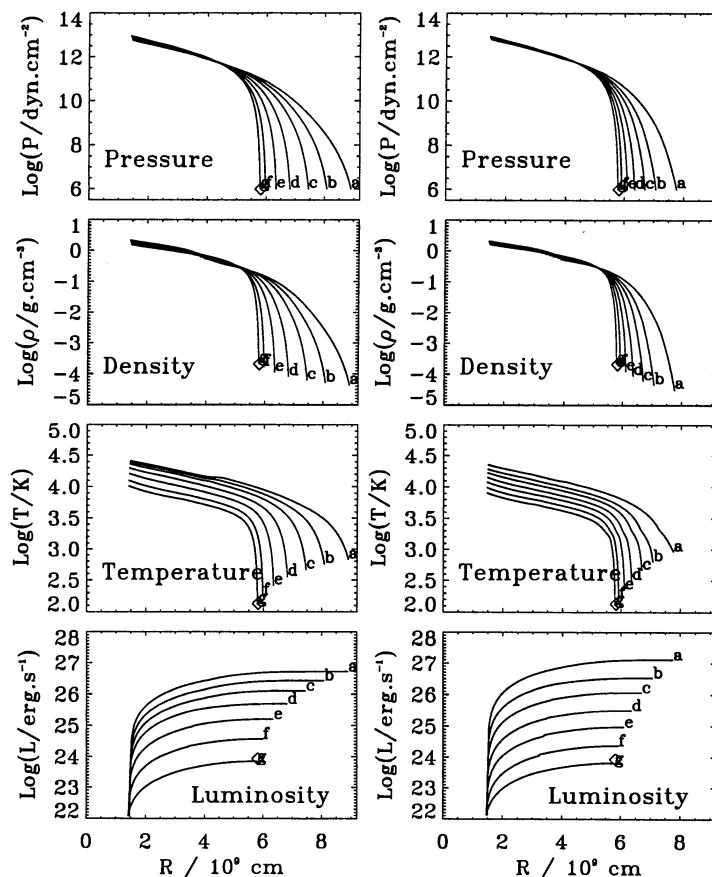


FIG. 3.—As Fig. 2 for evolutive models of Saturn. The different curves correspond to ages of (a) 0.001, (b) 0.01, (c) 0.03, (d) 0.1, (e) 0.3, (f) 1, and (g) 3 Gyr. Older models are not shown here since the planet becomes substantially cooler than observed actually after 3 Gyr and more.

see the signature of the fully convective metallic envelope, the PPT, the convective inner part of the molecular envelope, the radiative zone, and a convective external region which appears after 0.1 to 1 Gyr.

The evolution of the PPT toward the inner region of the

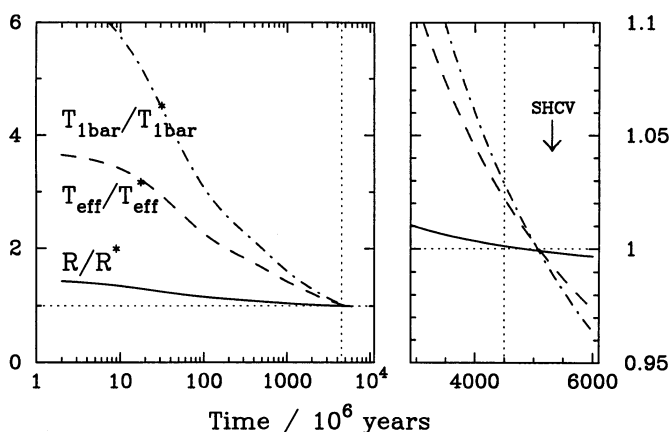


FIG. 4.—Contraction and cooling of an adiabatic model of Jupiter. The different curves represent the 1 bar temperature (dash-dots), the effective temperature (dash), and the mean radius (solid) as a function of the time. All these quantities are normalized to their present-day values: $T_{1\text{bar}}^*$, T_{eff}^* , and R^* . The right figure is an enlargement of the left figure. Note that the time is then represented on a linear scale. The dotted vertical line shows the age of the solar system (about 4.5 Gyr). The label “SHCV” indicates the age obtained by Saumon et al. (1992) for an adiabatic model of Jupiter.

planet (Figs. 8 and 9) shows that metallic hydrogen becomes progressively molecular. As shown by Saumon et al. (1992), the latent heat released during this transformation tends to increase the age of the model, but the effect remains small ($\sim 2\%$).

As shown on Figures 8 and 9, the difference between the entropy at the top of the radiative zone and the entropy at its bottom *decreases with time*. This is due to the fact that the density in the radiative region increases, as it is pushed down to deeper levels. In the mean time, the luminosity decreases,

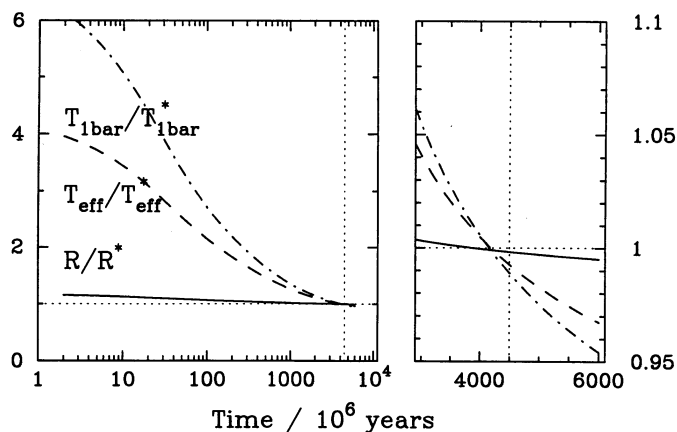


FIG. 5.—Contraction and cooling of a nonadiabatic model of Jupiter (see Fig. 4).

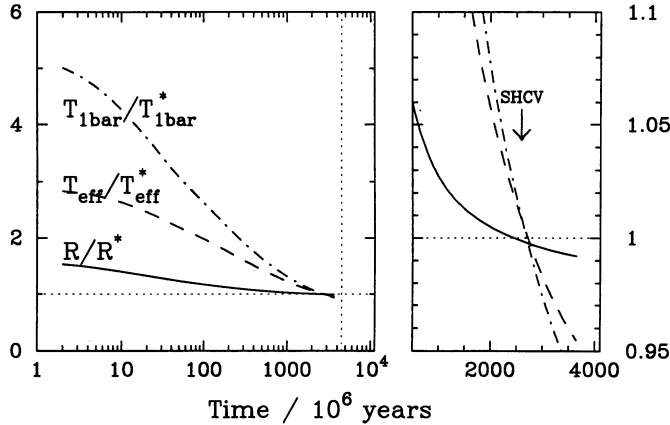


FIG. 6.—Contraction and cooling of an adiabatic model of Saturn. The label ‘SHCV’ indicates the age obtained by Saumon et al. (1992) for a similar model (see Fig. 4).

but not sufficiently rapidly. Then the ratio of the radiative to the adiabatic gradient *increases*.

Let us consider two adiabatic models separated by an unknown interval Δt_{ad} and two nonadiabatic models with the same external conditions but separated by Δt_{nad} . Let ΔS_{ad} and ΔS_{nad} be the entropy differences between each of these two models, respectively, below the eventual radiative region. Since this region contains most of the mass of the planet, we can estimate from equation (2) and the above discussion that

$$\Delta t_{nad} \approx \frac{M}{L} T_{nad} \Delta S_{nad} < \frac{M}{L} T_{ad} \Delta S_{ad} \approx \Delta t_{ad}, \quad (8)$$

where T_{ad} and $T_{nad} < T_{ad}$ are characteristic mean interior temperatures of the adiabatic and nonadiabatic models, respectively. This shows that the faster cooling of nonadiabatic models results from (i) the decrease with time of the entropy difference between the top and the bottom of the radiative region and (ii) the lower temperatures of nonadiabatic models.

The period during which fully convective models progressively become radiative is not observed here, probably because of the uncertainties on our opacity calculations at early epochs. For this early evolution phase, the cooling would be slower than for a fully convective planet, due to the larger entropy change. However, this is expected to occur well before the first

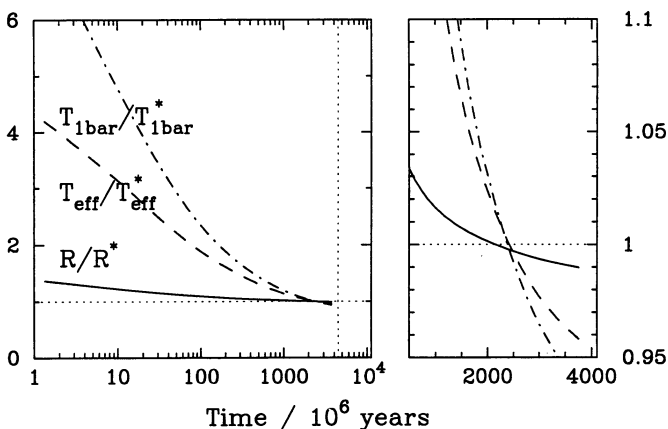


FIG. 7.—Contraction and cooling of a nonadiabatic model of Saturn (see Fig. 4).

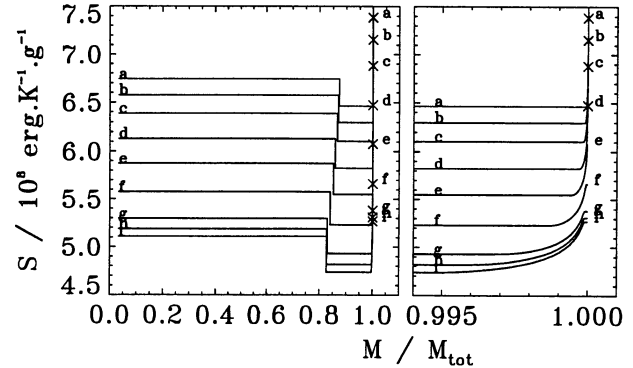


FIG. 8.—Specific entropy in function of the mass of a nonadiabatic model of Jupiter. As in Fig. 2, the labeled curves represent different ages from (a) 0.001 Gyr to (g) 6 Gyr. The crosses refer to the surface entropy. The discontinuity of S is due to the PPT. The presence of a radiative zone yields a diminution of the entropy. This region is enlarged on the right graph.

Gyr of evolution, and then to be unconsequential to the final results.

4. ON THE PRESENCE OF A HYDROGEN-HELIUM PHASE SEPARATION IN SATURN AND JUPITER

The observed abundance of helium in the atmosphere of Jupiter and Saturn is less than the protosolar value (see Gautier & Owen 1989). If we believe that the envelopes of the giant planets have been formed from hydrogen and helium present in the primitive nebula, i.e., with protosolar abundances, the missing quantity of helium at the surface must be somewhere inside the planet. It can be shown that gravitational settling by diffusion in a stable layer (e.g., in the radiative region) alone is highly inefficient for transporting helium from the surface to the interior (Guillot 1994). This is due to the fact that the microscopic diffusion is small ($D_m \approx 10^{-2} \text{ cm s}^{-1}$) compared to any turbulent diffusion (for example, turbulent diffusion due to meridional circulation in the radiative zone yields $D_T \approx 1 \text{ cm s}^{-1}$). Therefore, two explanations remain: the presence of a first-order transition, or a phase separation.

The presence of a first-order transition, like the PPT, yields a discontinuity of chemical composition in the two phases, according to the Gibbs phase rule (see Stevenson & Salpeter 1977; Hubbard 1989; Chabrier et al. 1992; Guillot et al. 1994b), so that the abundance of helium is different in the molecular and the metallic regions. The existence of such a

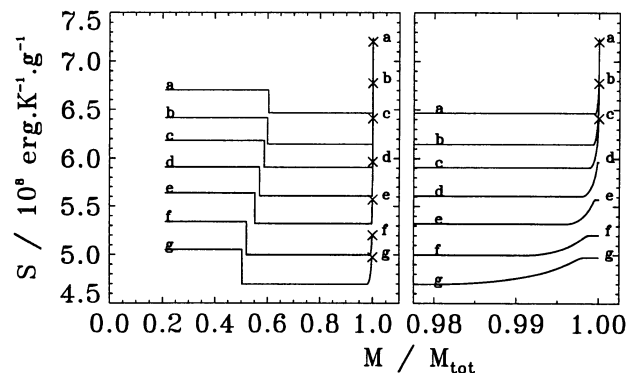


FIG. 9.—Specific entropy in function of the mass for a nonadiabatic model of Saturn, for ages between (a) 0.001 Gyr and (g) 3 Gyr (see Figs. 3 and 8).

PPT, though not demonstrated experimentally yet, is supported by the fact that when a continuous EOS is used, the optimized static models of Jupiter are in poor agreement with the observations, whereas a fair agreement is reached for static models calculated with a first-order transition (Chabrier et al. 1992; Guillot et al. 1994b). The problem is that, in order to explain the lack of helium in the atmosphere with respect to the protosolar abundance, the abundance of helium must be larger in the metallic than in the molecular region ($\Delta Y \equiv Y_{\text{met}} - Y_{\text{mol}} > 0$). Neither ΔY , nor its sign, can be determined accurately in the absence of a consistent hydrogen/helium EOS, taking into account the hydrogen-helium interactions. The actual H/He EOS is based on the so-called ideal-volume law (see Saumon et al. 1995). Smoluchowski (1967) and Stevenson & Salpeter (1977) advocate that, since helium is more soluble in molecular hydrogen than in metallic hydrogen, ΔY should be negative. If this could be proved, it would imply that the low atmospheric abundance of helium cannot be explained with this scenario, and that all the models of Jupiter (and Saturn) calculated until now are basically incorrect.

The second explanation is the presence of a hydrogen-helium phase separation, leading to a sedimentation of helium toward the interior of the planet and to the formation of a helium-rich layer surrounding the core. This requires, however, (i) that the internal temperature eventually becomes lower than the critical demixing temperature, and (ii) that the helium-rich droplets which form are not transported upward too efficiently by convection.

Figures 10 and 11 show isochrones for Jupiter and Saturn, respectively, in a temperature-pressure diagram, for both adia-

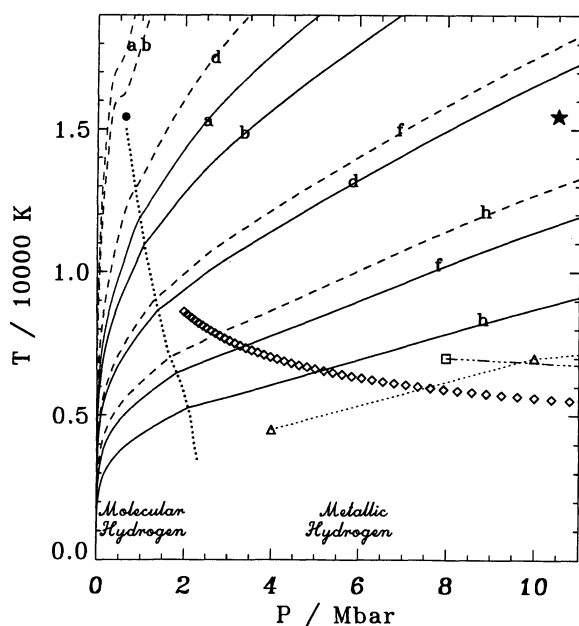


FIG. 10.—Isochrones for adiabatic (dashed lines), and nonadiabatic (solid lines) evolutionary models of Jupiter in a temperature-pressure diagram. As in Fig. 2, the labels correspond to the age of the models: (a) 0.001, (b) 0.01, (d) 0.1, (f) 1, and (h) 4.5 Gyr. The transition curve between molecular and metallic hydrogen (Saumon & Chabrier 1992) is shown as a dotted line. Other curves show the critical temperature of separation for a solar mixture of hydrogen and helium as predicted by: Stevenson (1982) (diamonds); Guillot & Chabrier (unpublished) (square and dash-triple dot line); Klepeis et al. (1991) (just one point: star); Pfaffenzeller et al. (1995) (triangles and thin dotted line). Helium separates out from hydrogen when and where the temperature profile is under the separation curve.

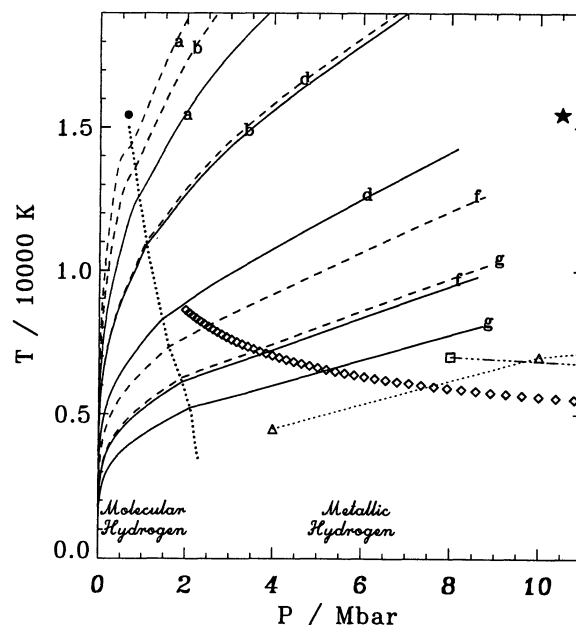


FIG. 11.—The interior of Saturn and the hydrogen-helium phase separation (see Fig. 10). Due to the presence of a heavy core in our models of Saturn (see Table 1), the core/envelope boundary is reached before 10 mbar.

batic (dashed line) and nonadiabatic (solid line) models. The figures also display various critical lines: the dotted line is the PPT critical line predicted by Saumon & Chabrier (1992), the diamond line is the He^{++} limit of solubility in H^+ predicted by Stevenson (1982), the dash-triple dot line shows the results from the same kind of calculations by Guillot & Chabrier (unpublished), the star is the helium limit of solubility in hydrogen predicted by Klepeis et al. (1991), whereas the triangles show the same limit with the new calculations of Pfaffenzeller, Hohn, & Ballone (1995). The major difference between the first type (Stevenson or Guillot & Chabrier), and the second type (Klepeis et al. or Pfaffenzeller et al.) of calculations is that the first ones assume a *fully ionized* mixture, whereas the second ones include a consistent treatment of the electronic structure around the nuclei, i.e., describe *partially ionized* plasmas. The most striking difference between these two kinds of calculations is the opposite sign for the slope of the critical demixing line. Whereas in the first scenario only a limited part of the metallic envelope experiences helium sedimentation, in the other schemes, if the phase separation occurs, it does so in most of the interior. The large difference between the Klepeis et al. and the Pfaffenzeller et al. calculations, both based on the same numerical scheme, show that the calculation of a phase diagram, which involves energy differences, is extremely sensitive on the input physics. Interestingly enough, if the PPT predicted by Saumon & Chabrier occurs in these planets, it is likely to occur *before* any hydrogen-helium phase separation along evolution (though the characteristics of the PPT, calculated for pure hydrogen, may be substantially modified when interactions with helium atoms are taken into account), so that hydrogen is likely to be ionized when the phase separation occurs. Figures 10 and 11 show the present limits of our understanding of critical phenomena in the interior of Jovian planets.

Once a phase separation occurs, Stevenson & Salpeter (1977) have shown that condition (ii) is probably satisfied.

5. CONCLUSION

We have calculated various evolutionary models for Jupiter and Saturn, either assuming convection throughout the entire planet, or taking into account the presence of a radiative window in the outermost part of each planet. The results for the adiabatic (i.e., fully convective) models confirm the previous conclusions of Saumon et al. (1992): The age found for an adiabatic model of Jupiter (5.1 Gyr) is too large compared to the age of the solar system (about 4.5 Gyr).

However, the presence of a radiative window, which is expected from the opacity calculations of Guillot et al. (1994a), drastically affects the evolution of these planets. The non-adiabatic models cool more rapidly than the adiabatic ones. This stems essentially from the facts that (i) radiative models always have smaller central temperatures than fully convective ones, since by definition, the radiative gradient is smaller than the adiabatic gradient in the radiative zone; (ii) the entropy change between the top and the bottom of the radiative zone decreases with time, as shown by Figures 8 and 9 (see also eq. [8]). For Jupiter, this leads to an age smaller than the age of the solar system (4.2 Gyr). This difference might be due to the underestimation of the opacities, or to inaccuracies in the surface boundary condition (eq. [4]).

On the other hand, if these two sources of uncertainty are not significant, an explanation of the observed internal heat flux is required. Since nonadiabatic models are significantly

cooler than adiabatic models, a hydrogen-helium phase separation process is likely to have started also in Jupiter. This provides the required source of internal energy—since helium droplets migrating toward the center of the planet liberate gravitational energy—as well as a consistent explanation for the low abundance of helium observed in the atmosphere of Jupiter ($Y = 0.18 \pm 0.04$), which is less than the solar value ($Y = 0.28$).

We find that adiabatic and nonadiabatic models of Saturn have an age significantly smaller than 4.5 billion years (2.6 Gyr and 2.4 Gyr, respectively). We conclude that an ongoing phase separation process is necessary to generate the observed internal energy, as indicated by previous studies.

The fact that the observed abundance of atmospheric helium is much smaller in Saturn ($Y = 0.06 \pm 0.05$) than in Jupiter suggests that the phase separation began earlier in Saturn, in agreement with the calculated ages mentioned above. We emphasize that the distribution of helium in the metallic region of this planet is probably strongly inhomogeneous. This stresses the need for further studies in this direction.

We thank D. Saumon for a careful reading of the manuscript and helpful comments, and P. Pellas for discussions. One of the authors (T. G.) gratefully acknowledges a postdoctoral fellowship from the European Space Agency.

APPENDIX

SEMIANALYTIC EVOLUTION MODEL

It is interesting, for the purpose of testing the validity of our numerical approach, and to better illustrate the physics involved in this problem, to derive a simple analytical model of evolution of giant planets. Such a model has been developed by Hubbard (1977) for Jupiter. Unfortunately, this model is not useful for testing the numerical calculations because of the physical assumptions made to solve the problem. Here, we adapt this model to the case of an ideal planet, which would obey entirely the classical perfect gas EOS and would be fully adiabatic.

These assumptions yield

$$T = T_1 \left(\frac{\rho}{\rho_1} \right)^\gamma, \quad (9)$$

where T_1 and ρ_1 are the temperature and the density at the 1 bar level, respectively, and the adiabatic coefficient

$$\gamma \equiv \left(\frac{\partial \ln T}{\partial \ln \rho} \right)_s, \quad (10)$$

is a constant and uniform quantity.

Let us assume moreover that the relation between the luminosity and the surface temperature has a simple form:

$$T_1 = B T_{\text{eff}}^a, \quad (11)$$

B and a being constant. Equation (4) is very close to this form, g being almost constant during the evolution.

The equation of conservation of energy (eq. [2]) can be integrated, using simple thermodynamic relations:

$$4\pi R_1^2 \sigma T_{\text{eff}}^4 = - \int_0^{M_{\text{tot}}} C_v \left(\frac{dT}{dt} - \gamma \frac{T}{\rho} \frac{d\rho}{dt} \right) dm. \quad (12)$$

On the other hand, equations (9) and (11) lead to

$$\frac{dT}{dt} = T \left[a(1 + \gamma) \frac{d \ln T_{\text{eff}}}{dt} + \gamma \frac{d \ln \rho}{dt} \right]. \quad (13)$$

This relation can be reported in equation (12), leading to the simple differential equation:

$$dt = -\alpha(T_{\text{eff}})T_{\text{eff}}^{a-5}dT_{\text{eff}}, \quad (14)$$

where

$$\alpha(T_{\text{eff}}) = \frac{Ba(1+\gamma)}{4\pi R_1^2 \sigma} C_v \int_0^{M_{\text{tot}}} \left(\frac{\rho}{\rho_1}\right)^\gamma dm. \quad (15)$$

Unfortunately, it is not possible to obtain an analytical form for $\alpha(T_{\text{eff}})$. However, we can easily bound the time elapsed to cool down from an effective temperature $T_{\text{eff},0}$ to an effective temperature $T_{\text{eff},1} < T_{\text{eff},0}$:

$$\frac{\alpha_{\min}}{4-a} (T_{\text{eff},1}^{a-4} - T_{\text{eff},0}^{a-4}) \leq \Delta t \leq \frac{\alpha_{\max}}{4-a} (T_{\text{eff},1}^{a-4} - T_{\text{eff},0}^{a-4}), \quad (16)$$

α_{\min} and α_{\max} being the extrema of $\alpha(T_{\text{eff}})$ on $(T_{\text{eff},0}, T_{\text{eff},1})$. This allows an estimation of the accuracy of the integration. With the code CEPAM, the relative error on a 5×10^9 yr evolution model with approximately 50 temporal time steps is less than 1%. This is smaller than any other source of uncertainty discussed in the text.

Hubbard (1977) shows that, since the evolution of Jupiter is governed by the evolution of the *metallic* region of the planet, and since the temperature in this region is such that $T \approx 18T_1 \rho^\gamma$, relation 14 is a good approximation. In this case, the form of α is slightly different:

$$\alpha(T_{\text{eff}}) = \frac{18}{4\pi R_1^2 \sigma} \int_0^{M_{\text{tot}}} a C_v \rho^\gamma dm.$$

With $q = 1.243$, $\gamma = 0.64$ and $C_v = 1.66k_B/m_H$, Hubbard (1977) obtains $\alpha = 2.79 \times 10^{23}$ cgs. Furthermore, it is easy to show that the time spent to cool down from an infinite temperature to $T_{\text{eff},1}$ is about 50 times smaller than the time spent to cool from $T_{\text{eff},1}$ to $T_{\text{eff},1}/4$. In other words, the evolution problem is not sensitive to the initial conditions. Thus, the uncertainties on the ages resulting from our choice of the initial conditions are smaller than 2%.

REFERENCES

- Barshay, S. S., & Lewis, J. S. 1978, *Icarus*, 33, 593
 Burrows, A., Hubbard, W. B., Saumon, D., & Lunine, J. I. 1993, *ApJ*, 406, 158
 Chabrier, G., Saumon, D., Hubbard, W. B., & Lunine, J. I. 1992, *ApJ*, 391, 817
 Fegley, B., Jr., & Lodders, K. 1994, *Icarus*, 110, 117
 Gautier, D., & Owen, T. 1989, in *Origin and Evolution of Planetary and Satellite Atmospheres*, ed. S. K. Atreya, J. B. Pollack, & M. S. Matthews (Tucson: Univ. Arizona Press), 487
 Göpel, C., Manhès, G., & Allègre, C. 1994, *Earth Planet. Sci. Lett.*, 121, 153
 Graboske, H. C., Pollack, J. B., Grossman, A. S., & Olness, R. J. 1975, *ApJ*, 199, 265
 Grossman, A. S., Pollack, J. B., Reynolds, R. T., Summers, A. L., & Graboske, H. C. 1980, *Icarus*, 42, 358
 Guillot, T. 1994, Ph.D. thesis, Université de Paris 7
 Guillot, T., Chabrier, G., Morel, P., & Gautier, D. 1994b, *Icarus*, 112, 354
 Guillot, T., Gautier, D., Chabrier, G., & Mosser, B. 1994a, *Icarus*, 112, 337
 Guillot, T., & Morel, P. 1995, *A&AS*, 109, 109
 Hayashi, C., Nakazawa, K., & Nakagawa, Y. 1985, in *Protostars & Planets II*, ed. D. C. Black & M. S. Matthews (Tucson: Univ. Arizona Press), 1100
 Holmes, N. C., Ross, M., & Nellis, W. J. 1995, *Phys. Rev. B*, in press
 Hubbard, W. B. 1977, *Icarus*, 30, 305
 ———. 1989, in *Origin and Evolution of Planetary and Satellite Atmospheres*, ed. S. K. Atreya, J. B. Pollack, & M. S. Matthews (Tucson: University of Arizona Press), 539
 Hubbard, W. B., & MacFarlane, J. J. 1980, *J. Geophys. Res.*, 85, 225
 Hubbard, W. B., & Marley, M. S. 1989, *Icarus*, 78, 102
 Hubbard, W. B., & Stevenson, D. J. 1984, in *Saturn*, ed. T. Gehrels & M. S. Matthews (Tucson: Univ. Arizona Press), 47
 Klepeis, J. E., Schafer, K. J., Barbee, T. W., & Ross, M. 1991, *Science*, 254, 986
 Lindal, G. F. 1992, *AJ*, 103, 967
 Lissauer, J. J. 1987, *Icarus*, 69, 249
 Pfaffenzeller, O., Hohn, D., & Ballone, P. 1995, *Phys. Rev. Letters*, 74, 2599
 Pollack, J. B., & Bodenheimer, P. 1989, in *Origin and Evolution of Planetary and Satellite Atmospheres*, ed. S. K. Atreya, J. B. Pollack, & M. S. Matthews (Tucson: Univ. Arizona Press), 564
 Pollack, J. B., Grossman, A. S., Moore, R., & Graboske, H. C. 1977, *Icarus*, 30, 111
 Safronov, V. S. 1972, in *Nice Symposium on the Origin of the Solar System*, ed. H. Reeves (Paris: Ed. CNRS)
 Safronov, V. S., & Ruzmaikina, T. V. 1985, in *Protostars & Planets II*, ed. D. C. Black, & M. S. Matthews (Tucson: Univ. Arizona Press), 959
 Saumon, D., & Chabrier, G. 1991, *Phys. Rev. A*, 44, 5122
 ———. 1992, *Phys. Rev. A*, 46, 2084
 Saumon, D., Chabrier, G., & Van Horn, H. M. 1995, *ApJS*, 99, 713
 Saumon, D., Hubbard, W. B., Chabrier, G., & Van Horn, H. M. 1992, *ApJ*, 391, 827
 Smoluchowski, R. 1967, *Nature*, 215, 691
 Stevenson, D. J. 1982, *Ann. Rev. Earth Planet. Sci.*, 10, 257
 Stevenson, D. J., & Salpeter, E. E. 1977, *ApJS*, 35, 239
 Wuchterl, G. 1991, *Icarus*, 91, 53